

Scalable Bayesian Inference for Generalized Linear Mixed Models via Stochastic Gradient MCMC

Samuel I. Berchuck*¹, Youngsoo Baek[†], Felipe A. Medeiros[‡], and Andrea Agazzi

Abstract. The generalized linear mixed model (GLMM) is widely used for analyzing correlated data, particularly in large-scale biomedical and social science applications. Scalable Bayesian inference for GLMMs is challenging because the marginal likelihood is intractable and conventional Markov chain Monte Carlo (MCMC) methods become computationally prohibitive as the number of subjects grows. We develop a stochastic gradient MCMC (SGMCMC) algorithm tailored to GLMMs that enables accurate posterior inference in the large-sample regime. Our approach uses Fisher’s identity to construct an unbiased Monte Carlo estimator of the gradient of the marginal log-likelihood, making SGMCMC feasible when direct gradient computation is impossible. We analyze the additional variability introduced by both minibatching and gradient approximation, and derive a post-hoc covariance correction that yields properly calibrated posterior uncertainty. Through simulations, we show that the proposed method provides accurate posterior means and variances, outperforming existing approaches, including control variate methods, in large- n settings. We further demonstrate the method’s practical utility in an analysis of electronic health records data, where accounting for variance inflation materially changes scientific conclusions.

MSC2020 subject classifications: Primary 62F15, 62R07; secondary 62J05.

Keywords: Scalable inference for dependent data, Big data, Uncertainty quantification, Variance correction, Monte Carlo gradient estimation, Fisher’s identity.

1 Introduction

Generalized linear mixed models (GLMMs) are widely used to model dependent data with clustered or repeated measures, particularly in biomedical and social sciences where such structures are common [1, 9]. By incorporating subject-specific random effects, GLMMs account for within-group correlation and support inference on both population- and subject-level parameters. Bayesian inference is especially attractive for GLMMs, offering coherent uncertainty quantification and flexible hierarchical modeling

arXiv: 2403.03007

*Department of Biostatistics & Bioinformatics, Department of Statistical Science, Duke University, sib2@duke.edu

†Department of Biostatistics & Bioinformatics, Duke University, youngsoo.baek@duke.edu

‡Department of Ophthalmology, University of Miami, fmedeiros@med.miami.edu

[§]Institute for Mathematical Statistics and Actuarial Sciences, Universität Bern, andrea.agazzi@unibe.ch

[20]. However, scalable Bayesian inference remains challenging due to the intractable marginal likelihood, which requires integrating over random effects. One could bypass this challenge by conditioning on the random effects and using standard Markov chain Monte Carlo (MCMC) techniques, since the conditional likelihood is tractable. But this approach becomes computationally infeasible, as the number of random effects increases with the sample size. Marginal likelihood-based approaches, including variational inference and stochastic gradient MCMC (SGMCMC), are scalable, but require evaluating or differentiating the marginal likelihood, which is intractable in GLMMs. Thus, GLMMs present a unique computational bottleneck: conditional methods are tractable but not scalable, and marginal methods are scalable but intractable. In this paper, we overcome the issue by introducing the first SGMCMC algorithm specifically tailored to GLMMs.

A critical challenge when using SGMCMC in practice is its tendency to produce inflated estimates of posterior variance. This error in posterior variance estimation is even more complex in the GLMM setting, and can be decomposed into two distinct sources. The first source is algorithmic and comes from data subsampling: for instance, stochastic gradient Langevin dynamics (SGLD) with a fixed step size (scaling in the sample size) targets a stationary distribution with an inflated variance [10]. Properties of variance correction strategies, such as control variates [4] or post-hoc bias correction [39], have not been studied in dependent-data settings. The second source is the statistical structure of GLMMs themselves: computing gradients of the marginal likelihood requires integrating over random effects, which is intractable in all but the simplest settings. We must approximate these gradients, injecting additional algorithmic noise beyond that introduced by minibatches. Together, these challenges highlight the need for scalable methods that carefully manage both algorithmic and statistical variance sources. Understanding how existing approaches handle these issues sheds light on the key design choices in our solution.

Most SGMCMC algorithms are based on Langevin-type diffusions, continuous-time stochastic differential equations (SDEs) whose stationary distribution coincides with the target Bayesian posterior [28]. These diffusions form the theoretical foundation for sampling algorithms that approximate Bayesian inference through stochastic dynamics. The foundational example is the SGLD algorithm, introduced by Welling and Teh [40], which replaces full-data gradients in Langevin dynamics with stochastic gradients computed from minibatches. While asymptotic consistency has been established for vanishing step-sizes [36], constant step-sizes are often used in practice for better mixing and computational efficiency [25]. However, this inflates the posterior variance relative to the true posterior [10], demonstrating the first source of the problem. A number of variance correction approaches have been proposed, including preconditioning [39, 34], stochastic gradient Hamiltonian Monte Carlo [12], Riemannian manifold extensions [30, 26] and control variate methods [4]. Of these, only the control variate method remain computationally comparable to the uncorrected SGLD, but its properties have not been evaluated in dependent data settings such as GLMMs. We address this challenge by introducing a novel, computationally efficient post-hoc correction of the algorithmic posterior samples with theoretical support. We demonstrate through simulated studies that our method yields an accurate approximation of the posterior

variance, while a naive use of control variates method in GLMMs can lead to both inflated and deflated variance estimates.

Numerous methods have been proposed to address the second challenge of approximating the marginal likelihood, including Laplace approximation [37], adaptive Gaussian-Hermite quadrature [27] and penalized quasi-likelihood [9]. All of them often struggle in high-dimensional or non-Gaussian random effects settings. Monte Carlo techniques [13, 19] and EM-based variants [7] offer more flexibility but can be computationally intensive and sensitive to tuning parameters. Bayesian methods, such as MCMC [20], INLA [32] and variational inference [29, 35], may be more scalable but still face challenges with large datasets and complex random effects structures. To avoid directly evaluating the marginal likelihood, we leverage Fisher's identity [17], which expresses the gradient of the marginal log-likelihood as an expectation over the conditional distribution of the random effects. This identity, previously used for variational inference in GLMMs [38], yields gradient estimators that naturally integrate with SGMCMC, and we build on this by developing a Monte Carlo approximation.

In this paper, we introduce the first SGLD-based algorithm tailored for scalable Bayesian inference in GLMMs. Our contributions are threefold: (i) a Monte Carlo gradient estimator based on Fisher's identity that enables SGMCMC in the presence of intractable marginal likelihoods; (ii) an asymptotic correction that adjusts for variance introduced by both minibatching and gradient approximation; and (iii) empirical results demonstrating accurate uncertainty quantification and substantial speedups over MCMC with the full dataset. The empirical comparison of our method with the control variate SGLD designed for independent data show that failing to account for the additional noise from likelihood approximation leads to biased uncertainty estimates, underscoring the need for methods built specifically for GLMMs.

2 Background and notation

We consider a database $\mathbf{Y} = (Y_1, \dots, Y_n)$ of size $n \in \mathbb{N}$, where Y_i represents the i -th observation for $i \in [n] := \{1, 2, \dots, n\}$. For population parameter $\boldsymbol{\Omega} \in \mathbb{R}^d$ we aim to estimate the posterior distribution, $\pi(\boldsymbol{\Omega}) := p(\boldsymbol{\Omega}|\mathbf{Y}) \propto p(\boldsymbol{\Omega}) \prod_{i=1}^n p(Y_i|\boldsymbol{\Omega})$, where $p(\boldsymbol{\Omega})$ is a prior distribution for the parameters $\boldsymbol{\Omega}$, $p(Y_i|\boldsymbol{\Omega})$ is the likelihood function and \propto denotes proportionality up to a constant. For notational convenience, we define $f_i(\boldsymbol{\Omega}) = -\log p(Y_i|\boldsymbol{\Omega})$ for all $i \in [n]$, $f_0(\boldsymbol{\Omega}) = -\log p(\boldsymbol{\Omega})$ and $f(\boldsymbol{\Omega}) = \sum_{i=0}^n f_i(\boldsymbol{\Omega})$. The posterior density can then be rewritten as, $\pi(\boldsymbol{\Omega}) \propto \exp\{-f(\boldsymbol{\Omega})\}$. We define the gradient of the marginal log-likelihood $g_i(\boldsymbol{\Omega}) = \nabla f_i(\boldsymbol{\Omega})$. It follows that the gradient of f is $\nabla f(\boldsymbol{\Omega}) = \nabla f_0(\boldsymbol{\Omega}) + \sum_{i=1}^n g_i(\boldsymbol{\Omega})$. We will use the notation $h_{\mathcal{S}}(\boldsymbol{\Omega}) = \frac{1}{S} \sum_{i \in \mathcal{S}} g_i(\boldsymbol{\Omega})$, where \mathcal{S} is a random subset of $[n]$ such that $|\mathcal{S}| = S$. We note that using this notation, the gradient of f can be written as $\nabla f(\boldsymbol{\Omega}) = \nabla f_0(\boldsymbol{\Omega}) + nh_{[n]}(\boldsymbol{\Omega})$.

2.1 Stochastic gradient Langevin dynamics

The Langevin diffusion, $\boldsymbol{\Omega}_t$, is defined by the SDE,

$$d\boldsymbol{\Omega}_t = -\nabla f(\boldsymbol{\Omega}_t) dt + \sqrt{2}d\mathbf{B}_t, \quad (1)$$

where $\nabla f(\boldsymbol{\Omega})$ denotes the gradient of f in $\boldsymbol{\Omega}$ and \mathbf{B}_t is a d -dimensional Brownian motion. Under mild regularity conditions on f , the stationary distribution of this diffusion is the posterior π , so that samples from π can be obtained from stationary trajectories of (1).

In practice, to sample from (1) we must discretize it. This can be done using the Euler-Maruyama approximation with step-size $\epsilon > 0$, whose update is given by

$$\boldsymbol{\Omega}_{k+1} = \boldsymbol{\Omega}_k - \epsilon \nabla f(\boldsymbol{\Omega}_k) + \sqrt{2\epsilon} \boldsymbol{\eta}_k, \quad \boldsymbol{\eta}_k \stackrel{iid}{\sim} \mathcal{N}_d(\mathbf{0}_d, \mathbf{I}_d). \quad (2)$$

The update of (2) has a computational cost that scales linearly in n . In the regime $n \gg 1$ (i.e., the big data regime of interest for this paper), this results in a prohibitive computational cost for the sampling process. In response to this observation, [40] introduced SGLD by replacing the full-data gradient $\nabla f(\boldsymbol{\Omega})$ with an unbiased estimate $\nabla \hat{f}_{SGLD}(\boldsymbol{\Omega}) = \nabla f_0(\boldsymbol{\Omega}) + \frac{n}{S} \sum_{i \in \mathcal{S}} \nabla f_i(\boldsymbol{\Omega}) = \nabla f_0(\boldsymbol{\Omega}) + nh_{\mathcal{S}}(\boldsymbol{\Omega})$, where \mathcal{S} is a random subset of $[n]$ drawn *iid* at each iteration with $|\mathcal{S}| = S$. The minibatch estimator $h_{\mathcal{S}}(\boldsymbol{\Omega})$ can easily be seen to be an unbiased estimator of the full-data gradient $h_{[n]}(\boldsymbol{\Omega})$. When $S \ll n$, this significantly reduces the cost of the gradient computation. A single update of the SGLD algorithm is thus given by,

$$\boldsymbol{\Omega}_{k+1} = \boldsymbol{\Omega}_k - \epsilon \nabla \hat{f}_{SGLD}(\boldsymbol{\Omega}_k) + \kappa \sqrt{2\epsilon} \boldsymbol{\eta}_k, \quad (3)$$

where $\kappa = 1$ and $\epsilon > 0$. [40] demonstrated that with vanishing step-size, SGLD permits samples from the posterior π , however in practice this has proven difficult and inference using SGLD is often done using a fixed step-size, meaning the resulting posterior has an inflated variance [10]. The case $\kappa = 0$, where the minibatch randomness is the only source of noise, corresponds to stochastic gradient descent (SGD). While SGLD and its simpler variant, SGD, are widely used for independent data, their application to dependent-data models like GLMMs is limited by the intractability of the marginal log-likelihood. In particular, $h_{\mathcal{S}}(\boldsymbol{\Omega})$ can no longer be computed, because $\nabla f_i(\boldsymbol{\Omega})$ cannot be found in closed form. We now introduce GLMM notation and describe how SGLD must be adapted for this setting.

2.2 Generalized linear mixed model

In GLMM, each subject $i \in [n]$ has $n_i \in \mathbb{N}$ repeated measures, Y_{it} for $t \in [n_i]$. Let \mathbf{x}_{it} denote a p -dimensional vector of covariates, and \mathbf{z}_{it} denote a q -dimensional vector of covariates that are assumed to have subject-specific parameters. The elements of $\mathbf{Y}_i = (Y_{i1}, \dots, Y_{in_i})^\top$ are modeled as conditionally independent random variables from the exponential family,

$$p(Y_{it} | \theta_{it}, \phi) = \exp \left\{ \frac{Y_{it}\theta_{it} - b(\theta_{it})}{a(\phi)} + c(Y_{it}, \phi) \right\},$$

where θ_{it} is a canonical parameter related to the linear predictor $\eta_{it} = \mathbf{x}_{it}^\top \boldsymbol{\beta} + \mathbf{z}_{it}^\top \boldsymbol{\gamma}_i$. The parameter $\boldsymbol{\beta}$ is a p -dimensional vector of population regression parameters (sometimes referred to as fixed effects) and $\boldsymbol{\gamma}_i$ is a q -dimensional vector of subject-specific parameter

deviations from the population parameters (sometimes referred to as random effects). The subject-specific parameters are assumed to have the following distribution, $\gamma_i \stackrel{iid}{\sim} \mathcal{N}_q(0, \Sigma)$, although our method generalizes naturally outside this setting. The parameter ϕ is an m -dimensional dispersion vector and $a(\cdot), b(\cdot), c(\cdot)$ are known functions that output a scalar. The canonical link function, $d(\cdot)$, is obtained when $\theta_{it} = \eta_{it}$ which is when $d(\mu_{it}) = \theta_{it}$, where $\mu_{it} = \mathbb{E}[Y_{it}|\beta, \gamma_i, \phi]$. Population parameters are grouped as $\Omega = (\beta, \Sigma, \phi)$.

We are interested in the posterior distribution, $p(\Omega|\mathbf{Y})$, where $\mathbf{Y} = (\mathbf{Y}_1^\top, \dots, \mathbf{Y}_n^\top)^\top$. The posterior is proportional to the marginal joint likelihood times the prior, $\pi(\Omega) := p(\Omega|\mathbf{Y}) \propto p(\mathbf{Y}|\Omega)p(\Omega)$, where we assume that the prior and likelihood decompose as $p(\Omega) = p(\beta)p(\Sigma)p(\phi)$ and $p(\mathbf{Y}|\Omega) = \prod_{i=1}^n p(\mathbf{Y}_i|\Omega)$. The subject-specific likelihood contribution is given by the following q -dimensional integral that in general is intractable,

$$p(\mathbf{Y}_i|\Omega) = \int \prod_{t=1}^{n_i} p(Y_{it}|\beta, \gamma_i, \phi) p(\gamma_i|\Sigma) d\gamma_i. \quad (4)$$

In rare exceptions, such as when the random effects are Gaussian and conjugate to the likelihood, the marginal likelihood admits a closed-form expression. However, in most practical GLMMs, this integral is analytically intractable due to the non-Gaussian structure of the random effects or the nonlinearity of the link function. As a result, computing or even differentiating the marginal log-likelihood requires approximation. This presents a fundamental challenge: without access to exact gradients, gradient-based inference methods such as SGLD cannot be directly applied.

To address this limitation, we turn to Fisher's identity [17],

$$g_i(\Omega) = \mathbb{E}_{\gamma_i|\mathbf{Y}_i, \Omega} [-\nabla \log p(\mathbf{Y}_i, \gamma_i|\Omega)], \quad (5)$$

recalling that $g_i(\Omega) = \nabla f_i(\Omega) = -\nabla \log p(\mathbf{Y}_i|\Omega)$. Fisher's identity re-writes the marginal log-likelihood as an expectation with respect to the posterior distribution of the subject-specific parameters, $p(\gamma_i|\mathbf{Y}_i, \Omega)$. Fisher's identity has a long history in models with latent variables, including linear dynamic systems [33], non-linear and non-Gaussian state space models [24], and high-dimensional inverse problems [23]. Tran et al. [38] applied it to GLMMs in a variational inference framework incorporating neural networks. Their method estimated conditional log-likelihood gradients via backpropagation and approximated expectations using importance sampling. However, it relied on a Gaussian variational family, and the uncertainty in estimating $g_i(\Omega)$ was not propagated into the posterior. In our approach, we introduce a Monte Carlo estimator for $g_i(\Omega)$ based on Fisher's identity and incorporate it into an SGMCMC algorithm that permits full Bayesian inference that scales to large datasets while preserving uncertainty quantification. When used with independent Monte Carlo samples to approximate $g_i(\Omega)$, our approach yields unbiased stochastic gradients of the marginal log-likelihood, enabling SGLD updates for models with intractable marginal gradients.

3 SGMCMC for GLMMs

We now introduce our SGMCMC algorithm for scalable Bayesian inference in GLMMs. Our approach builds on Fisher's identity to construct a Monte Carlo estimator of the gradient of the marginal log-likelihood, enabling the use of SGLD in this otherwise intractable setting. The SGLD algorithm from [40] given in (3) approximates the full-data gradient, $\nabla f(\boldsymbol{\Omega}) = \nabla f_0(\boldsymbol{\Omega}) + nh_{[n]}(\boldsymbol{\Omega})$, with an unbiased estimator $\nabla \hat{f}_{SGLD}(\boldsymbol{\Omega}) = \nabla f_0(\boldsymbol{\Omega}) + nh_{\mathcal{S}}(\boldsymbol{\Omega})$. The estimator from [40] relies on a vanishing step-size and the fact that $\nabla f_i(\boldsymbol{\Omega})$ can be computed. In this section, we introduce the following fixed step-size SGLD algorithm for GLMMs,

$$\nabla \hat{f}_{GLMM}(\boldsymbol{\Omega}) = \nabla f_0(\boldsymbol{\Omega}) + \frac{n}{S} \sum_{i \in \mathcal{S}} \hat{g}_i(\boldsymbol{\Omega}) = \nabla f_0(\boldsymbol{\Omega}) + nh_{\mathcal{S}}(\boldsymbol{\Omega}). \quad (6)$$

Our estimator is a function of a *population* estimator $\hat{h}_{\mathcal{S}}(\boldsymbol{\Omega}) = \frac{1}{S} \sum_{i \in \mathcal{S}} \hat{g}_i(\boldsymbol{\Omega})$, which is a minibatch average of the subject-specific gradient estimators, $\hat{g}_i(\boldsymbol{\Omega})$. Recall that $g_i(\boldsymbol{\Omega}) = \nabla f_i(\boldsymbol{\Omega}) = -\nabla \log p(\mathbf{Y}_i | \boldsymbol{\Omega})$ is the gradient of the marginal log-likelihood for subject i , and in the GLMM setting must be approximated. In Section 3.1, we formally define an estimator for $g_i(\boldsymbol{\Omega})$ and derive its statistical properties. Furthermore, we characterize the *population* estimator $\hat{h}_{\mathcal{S}}(\boldsymbol{\Omega})$, show that it is an unbiased estimator of $h_{[n]}(\boldsymbol{\Omega})$, and introduce an estimator for its covariance. In Section 3.2, we derive a post-hoc correction for the posterior samples obtained from the algorithm in (6) run with a fixed step-size. Finally, in Section 3.3, we detail the practical implementation of the algorithm, providing a step-by-step procedure for inference.

3.1 Deriving an estimator for the marginal likelihood

We begin by defining the estimator for $g_i(\boldsymbol{\Omega})$. As given in (5), we use Fisher's identity to re-write $g_i(\boldsymbol{\Omega})$ as an expectation with respect to the posterior distribution of the random effects. Equation (5) can be decomposed to reveal that the gradient inside the expectation is computed on two distributions that are explicitly defined for GLMMs, namely the conditional likelihood and the distribution for the random effects,

$$g_i(\boldsymbol{\Omega}) = \mathbb{E}_{\boldsymbol{\gamma}_i | \mathbf{Y}_i, \boldsymbol{\Omega}} [-\nabla \log p(\mathbf{Y}_i | \boldsymbol{\gamma}_i, \boldsymbol{\beta}, \boldsymbol{\phi}) - \nabla \log p(\boldsymbol{\gamma}_i | \boldsymbol{\Sigma})]. \quad (7)$$

Both the conditional likelihood, $p(\mathbf{Y}_i | \boldsymbol{\gamma}_i, \boldsymbol{\beta}, \boldsymbol{\phi})$, and the random effects distribution, $p(\boldsymbol{\gamma}_i | \boldsymbol{\Sigma})$, are members of the exponential family and are differentiable under mild conditions. Note that the density of the random effects distribution is not required to be a member of the exponential family, but only to have a closed-form density that is differentiable.

The representation of the gradient of the marginal log-likelihood as an expectation in (7) motivates a Monte Carlo estimator for $g_i(\boldsymbol{\Omega})$, as in [38]. We define our Monte Carlo estimator based on R samples of $\boldsymbol{\gamma}_i$ as,

$$\hat{g}_i(\boldsymbol{\Omega}) = -\frac{1}{R} \sum_{r=1}^R \nabla \log p(\mathbf{Y}_i, \boldsymbol{\gamma}_{ir} | \boldsymbol{\Omega}), \quad \boldsymbol{\gamma}_{ir} \stackrel{iid}{\sim} p(\boldsymbol{\gamma}_i | \mathbf{Y}_i, \boldsymbol{\Omega}). \quad (8)$$

For the rest of this section, and in the theoretical analysis of Section 3.2, we will assume that we can draw *iid* Monte Carlo samples from the underlying conditional distribution $p(\gamma_i | \mathbf{Y}_i, \Omega)$. The impact of using biased sampling methods (e.g., MCMC that only yields exact samples in the ergodic limit) or other approximations of $p(\gamma_i | \mathbf{Y}_i, \Omega)$ and the corresponding posterior variance will be discussed in Section 3.3. With this caveat, the stochastic gradient estimator from (8) is straightforward to compute, since the gradient, $\nabla \log p(\mathbf{Y}_i, \gamma_{ir} | \Omega)$, is analytically available. The covariance of the Monte Carlo estimator (8) is defined as,

$$\Psi_i(\Omega) = \mathbb{V}_{\gamma_i | \mathbf{Y}_i, \Omega}(\hat{g}_i(\Omega)) = \frac{1}{R} \mathbb{V}_{\gamma_i | \mathbf{Y}_i, \Omega}(\nabla \log p(\mathbf{Y}_i, \gamma_i | \Omega)), \quad (9)$$

where $\mathbb{V}_{\mathbf{X} | \mathbf{Y}}(f(\mathbf{X}))$ is the conditional covariance of $f(\mathbf{X})$ given \mathbf{Y} . The associated empirical covariance is given by,

$$\hat{\Psi}_i(\Omega) = \frac{1}{R(R-1)} \sum_{r=1}^R (\nabla \log p(\mathbf{Y}_i, \gamma_{ir} | \Omega) - \hat{g}_i(\Omega)) (\nabla \log p(\mathbf{Y}_i, \gamma_{ir} | \Omega) - \hat{g}_i(\Omega))^{\top}. \quad (10)$$

From the form of the covariance of the Monte Carlo estimator in (10), we see that $\hat{\Psi}_i(\Omega)$ is minimized as $R \rightarrow \infty$ and with improved concentration of the joint distribution, reflecting two axes of precision: algorithmic (sampling) and statistical (model-based). The following lemma shows that the Monte Carlo estimator and its empirical covariance are unbiased.

Lemma 3.1. *For all $i \in [n]$, $\hat{g}_i(\Omega)$ as defined in (8) and $\hat{\Psi}_i(\Omega)$ as defined in (9) are unbiased estimators of the gradient of the marginal log-likelihood, $g_i(\Omega)$, and the covariance matrix $\Psi_i(\Omega)$, respectively.*

Proof. The proof is given in Section 1 of the online supplementary materials [5]. \square

Having defined an estimator for $g_i(\Omega)$, we proceed to study the statistical properties of the minibatch estimate of the *population* gradient, $\hat{h}_{\mathcal{S}}(\Omega)$. In doing so, we account for the uncertainty from (i) sampling a minibatch, and (ii) the Monte Carlo estimator as defined in Lemma 3.1. The statistical properties are given in the following lemma.

Lemma 3.2. *For every $\Omega \in \mathbb{R}^d$, $\hat{h}_{\mathcal{S}}(\Omega)$ is an unbiased estimator of $h_{[n]}(\Omega)$ with covariance $S^{-1}\Psi(\Omega)$ and $\Psi(\Omega) = n^{-1} \sum_{i=1}^n (g_i(\Omega) - h_{[n]}(\Omega)) (g_i(\Omega) - h_{[n]}(\Omega))^{\top} + \Psi_i(\Omega)$. Finally,*

$$\begin{aligned} \hat{\Psi}(\Omega) &:= \frac{1}{n} \sum_{i=1}^n (\hat{g}_i(\Omega) - \hat{h}_{[n]}(\Omega)) (\hat{g}_i(\Omega) - \hat{h}_{[n]}(\Omega))^{\top} + \frac{\hat{\Psi}_i(\Omega)}{n}, \\ &= \frac{1}{n} \sum_{i=1}^n (\hat{g}_i(\Omega) - \hat{h}_{[n]}(\Omega)) (\hat{g}_i(\Omega) - \hat{h}_{[n]}(\Omega))^{\top} + \frac{1}{n^2} \sum_{i=1}^n \hat{\Psi}_i(\Omega), \end{aligned}$$

is an unbiased estimator of $\Psi(\Omega)$, where $\hat{h}_{[n]}(\Omega) = \frac{1}{n} \sum_{i=1}^n \hat{g}_i(\Omega)$.

Proof. The proof is given in Section 2 of the online supplementary materials [5]. \square

The covariance for $\hat{h}_S(\Omega)$ is given by $S^{-1}\Psi(\Omega)$ and becomes smaller with increases in minibatch size ($S \rightarrow n$). The estimator for $\Psi(\Omega)$, $\hat{\Psi}(\Omega)$, can be decomposed into two distinct components reflecting different sources of uncertainty. The first component arises from Monte Carlo estimation error at the subject level. Since each individual gradient $\hat{g}_i(\Omega)$ is estimated via Monte Carlo sampling, the average gradient $\hat{h}_S(\Omega)$ inherits this noise, contributing a variance term that sums the Monte Carlo variances for subject i , $\hat{\Psi}_i(\Omega)$, and that scales as n^{-2} . This term vanishes rapidly with increasing sample size or more accurate subject-level estimation, and may become negligible in large-scale applications. The second, dominant term captures variability across subjects in their true gradients and reflects the statistical uncertainty in estimating the population mean gradient, $h_{[n]}(\Omega)$. This component scales as n^{-1} , and persists even with perfect Monte Carlo estimates. Together, these terms describe how both within-subject estimation error and between-subject heterogeneity contribute to the uncertainty in the overall gradient estimator. Having defined our estimators, we can formally write the update of our SGLD algorithm as follows,

$$\Omega_{k+1} = \Omega_k - \epsilon \nabla \hat{f}_{GLMM}(\Omega) + \kappa \sqrt{2\epsilon} \eta_k \quad (11)$$

where $\nabla \hat{f}_{GLMM}(\Omega)$ is defined in (6) and $\hat{g}_i(\Omega)$ and $\hat{h}_S(\Omega)$ in Lemma 3.1 and 3.2.

3.2 Variance correction for SGLD

We can use the statistical characterization of the gradient estimators in Section 3.1 to rewrite our SGLD algorithm, exposing the noise added by approximations. By adding and subtracting the full-data gradient to (11) we obtain,

$$\Omega_{k+1} = \Omega_k - \epsilon \nabla f(\Omega_k) + \sqrt{2\epsilon} \left(\sqrt{\frac{\epsilon n^2}{2S}} \xi(\Omega_k) + \kappa \eta_k \right), \quad (12)$$

where $\xi(\Omega)$ is a set of random variables independent of η with mean zero and covariance $\mathbb{V}(\xi(\Omega)) = \Psi(\Omega)$. The sum of the two independent variance terms is given by, $\Gamma(\Omega) = \epsilon n^2 \Psi(\Omega) / (2S) + \kappa \mathbf{I}_d$. Note that (12) is identical to the full-data gradient Euler-Maruyama discretization of Langevin diffusion given in (2), with the approximation noise isolated to the $\xi(\Omega)$ term. This indicates that our algorithm will return unbiased posterior samples with inflated variance, but gives us clues on how to reduce the variance inflation. The most straightforward option is to choose either $\epsilon \approx n^{-2}$ or $S \approx n$, but it cancels out any computational benefits of subsampling the data. In this section, we instead introduce an approach for correcting the posterior variance estimate based on asymptotic analysis.

Heuristic Argument

To discuss the asymptotic properties of the quantities of interest in the relevant regime $n \rightarrow \infty$, we introduce a few notations. For two sequences $\{a_n\}_n$, $\{g_n\}_n$, $g_n = O_n(a_n)$,

$g_n = \Omega_n(a_n)$ means that there exists $C > 0$ for which $\|g_n\| \leq Ca_n$ and $\|g_n\| \geq Ca_n$, respectively, as $n \rightarrow \infty$. For a $d \times d$ -dimensional real matrix \mathbf{M} , we use the operator norm: $\|\mathbf{M}\| = \sup_{\mathbf{v} \in \mathbb{R}^d: \|\mathbf{v}\|=1} \|\mathbf{M}\mathbf{v}\|$.

We start by approximating the discrete-time update in (12) with a forward Euler-Maruyama update of matching mean and covariance,

$$\boldsymbol{\Omega}_{k+1} - \boldsymbol{\Omega}_k = -\epsilon \nabla f(\boldsymbol{\Omega}_k) + \sqrt{2\epsilon} \boldsymbol{\eta}'_k, \quad \boldsymbol{\eta}'_k \sim \mathcal{N}(\mathbf{0}, \boldsymbol{\Gamma}(\boldsymbol{\Omega}_k)),$$

where $\boldsymbol{\Gamma}(\boldsymbol{\Omega}) = \epsilon n^2 \boldsymbol{\Psi}(\boldsymbol{\Omega})/(2S) + \kappa \mathbf{I}_d$. The update approximates the evolution of the SDE, $d\boldsymbol{\Omega}_t = -\nabla f(\boldsymbol{\Omega}_t)dt + \sqrt{2\sigma(\boldsymbol{\Omega}_t)}d\mathbf{B}_t$ for $\sigma(\boldsymbol{\Omega})\sigma(\boldsymbol{\Omega})^\top = \boldsymbol{\Gamma}(\boldsymbol{\Omega})$. By the law of large numbers, we expect $n^{-1}\nabla f(\boldsymbol{\Omega})$ to converge to an n -independent function of $\boldsymbol{\Omega}$ so that $\nabla f(\boldsymbol{\Omega}) = \Omega_n(n)$ for $\boldsymbol{\Omega} \neq \boldsymbol{\Omega}^*$. Consequently, the distribution of $\boldsymbol{\Omega}_t$ will concentrate around the minimizer $\boldsymbol{\Omega}^*$ of f justifying the linearization of the SDE approximation of the update around $\boldsymbol{\Omega}^*$,

$$d(\boldsymbol{\Omega}_t - \boldsymbol{\Omega}^*) = -\nabla^2 f(\boldsymbol{\Omega}^*)(\boldsymbol{\Omega}_t - \boldsymbol{\Omega}^*)dt + \sqrt{2\sigma(\boldsymbol{\Omega}^*)}d\mathbf{B}_t.$$

The invariant measure of this linear equation can be explicitly computed as $\bar{\pi}(\boldsymbol{\Omega}) = Z^{-1} \exp \{-(\boldsymbol{\Omega} - \boldsymbol{\Omega}^*)^\top \boldsymbol{\Sigma}^{-1}(\boldsymbol{\Omega} - \boldsymbol{\Omega}^*)/2\}$, where $\boldsymbol{\Sigma}$ satisfies the Lyapunov equation,

$$\mathbf{A}\boldsymbol{\Sigma} + \boldsymbol{\Sigma}\mathbf{A}^\top = 2\boldsymbol{\Gamma}, \tag{13}$$

for $\mathbf{A} = \nabla^2 f(\boldsymbol{\Omega}^*)$ and $\boldsymbol{\Gamma} = \epsilon n^2 \boldsymbol{\Psi}(\boldsymbol{\Omega}^*)/(2S) + \kappa \mathbf{I}_d$. Since both $\boldsymbol{\Sigma}$ and \mathbf{A} are symmetric, (13) can be written as $\boldsymbol{\Sigma}\mathbf{A} + \mathbf{A}\boldsymbol{\Sigma} = 2\boldsymbol{\Gamma}$. Solving this equation for \mathbf{A} , where $\boldsymbol{\Sigma}, \boldsymbol{\Gamma}$ are estimated from SGLD samples, yields an accurate estimate of the desired covariance.

Remark 3.3. Note that, whenever $\epsilon/S = \Omega_n(n^{-2+\delta})$ for any $\delta > 0$, the contribution $\kappa \mathbf{I}_d$ of the injected noise from the Langevin dynamics becomes negligible with respect to the one resulting from the minibatch stochastic approximation of the gradient. In this sense, analyzing SGD or SGLD ($\kappa = 0$ or $\kappa = 1$) results in the same leading order asymptotics.

Asymptotic Analyses

We now verify the above heuristic insight against asymptotic expansions related to the Lyapunov solution (13). Throughout, we rely on the estimates of [10] for SGLD, derived through simple coupling arguments and Taylor expansion. First, we state the following assumption commonly made in log-concave sampling literature.

Assumption 1. *For all $j \in \{0\} \cup [n]$, f_j is convex, is four times continuously differentiable and there exists an $O_n(1)$ constant $L > 0$ such that for all $\ell \in \{2, 3, 4\}$ it holds that $\sup_{\boldsymbol{\Omega}} \|D^\ell f_j(\boldsymbol{\Omega})\| \leq L$. Furthermore, we assume that f is M -strongly convex (i.e., for any $\boldsymbol{\Omega}, \boldsymbol{\Omega}' \in \mathbb{R}^d$ we have $\langle g(\boldsymbol{\Omega}) - g(\boldsymbol{\Omega}'), \boldsymbol{\Omega} - \boldsymbol{\Omega}' \rangle \geq M\|\boldsymbol{\Omega} - \boldsymbol{\Omega}'\|^2$).*

The assumption yields a few consequences. First, for all $j \in [n]$, g_j is L -Lipschitz continuous: for all $\boldsymbol{\Omega}, \boldsymbol{\Omega}'$ we have $\|g_j(\boldsymbol{\Omega}) - g_j(\boldsymbol{\Omega}')\| \leq L\|\boldsymbol{\Omega} - \boldsymbol{\Omega}'\|$ and also $\|g(\boldsymbol{\Omega}) - g(\boldsymbol{\Omega}')\| \leq (n+1)L\|\boldsymbol{\Omega} - \boldsymbol{\Omega}'\|$. Second, f has a unique minimizer, which will be denoted as $\boldsymbol{\Omega}^*$ throughout.

We report the following result from [10, Lemma 1], adapting its notation. This result establishes existence and uniqueness of an invariant measure for the process Ω_k from (3) and geometric convergence of the distribution of Ω_k to such invariant measure. Here, we denote by $\mathcal{P}_2(\mathbb{R}^d)$ the space of probability measures on \mathbb{R}^d with finite second moments, by $W_2^2(\mu, \nu)$ the Wasserstein 2-distance between $\mu, \nu \in \mathcal{P}^2$ and by $P_k(\Omega_0, \cdot) = \mathbb{P}(\Omega_k \in \cdot)$ the distribution of Ω_k with initial condition Ω_0 .

Lemma 3.4. *Under Assumption 1, for any step size $\epsilon \in (0, 2(Ln)^{-1})$, Ω_k defined as in (3) has a unique invariant measure $\tilde{\pi} \in \mathcal{P}_2(\mathbb{R}^d)$. In addition, for all $\epsilon \in (0, 1/(Ln)^{-1}]$, $\Omega_0 \in \mathbb{R}^d$ and $k \in \mathbb{N}$, we have that,*

$$W_2^2(P_k(\Omega_0, \cdot), \tilde{\pi}) \leq (1 - M\epsilon)^k \int_{\mathbb{R}^d} \|\Omega_0 - \Omega\|^2 \tilde{\pi}(d\Omega).$$

Note that the above result confirms the natural intuition about MCMC: sampler mixes faster towards stationarity with larger $\epsilon > 0$, up to the order of n^{-1} , a threshold for guaranteed algorithmic stability. On the other hand, we aim to approximate the underlying posterior distribution, not the invariant distribution $\tilde{\pi}$ of SGLD which is biased due to algorithmic noise. Intuitively, by a Laplace-type argument, it must be the case that the posterior covariance $\int_{\mathbb{R}^d} (\Omega - \Omega^*)^{\otimes 2} \pi(d\Omega)$ should be similar to the inverse of $\mathbf{A} = \nabla^2 f(\Omega^*)$ for large n . We cite the following result for our context, whose proof is reported in [10]. Note that both the posterior covariance and \mathbf{A}^{-1} are $O_n(n^{-1})$ under Assumption 1, since the Lipschitz constant $L = O_n(1)$.

Proposition 3.5. *Let Assumption 1 hold and assume that $\liminf_{n \rightarrow \infty} n^{-1} M > 0$. Then,*

$$\int_{\mathbb{R}^d} (\Omega - \Omega^*)^{\otimes 2} \pi(d\Omega) = \nabla^2 f(\Omega^*)^{-1} + O_n(n^{-3/2}),$$

and,

$$\int_{\mathbb{R}^d} \Omega \pi(d\theta) - \Omega^* = -\frac{1}{2} \nabla^2 f(\Omega^*)^{-1} D^3 f(\Omega^*) [\nabla^2 f(\Omega^*)^{-1}] + O_n(n^{-3/2}).$$

Finally, we now show that using the tools already used in the previous analysis [10], the covariance $\Sigma := \int_{\mathbb{R}^d} (\Omega - \Omega^*)^{\otimes 2} \tilde{\pi}(d\Omega)$ can be related to \mathbf{A} through the Lyapunov equation (13). Since, according to the following theorem, the matrix \mathbf{A} “almost solves” the Lyapunov equation, the heuristic argument that the solution of this equation yields an order-wise correct posterior covariance can be justified in the large- n regime.

Theorem 3.6. *Let Assumption 1 hold and recall the definition $\mathbf{A} := \nabla^2 f(\Omega^*)$. Set $\epsilon = Sn^{-(1+\delta)}$ for a $\delta \in (0, 1]$ and assume that $\liminf_{n \rightarrow +\infty} nM^{-1} > 0$. Then,*

$$\Sigma \mathbf{A} + \mathbf{A} \Sigma = 2\Gamma \left(1 + O_n(n^{-\delta/2}) \right).$$

Proof. The proof is given in Section 3 of the online supplementary materials [5]. \square

3.3 Practical implementation of the algorithm

Description of the Correction Algorithm

Using the SGLD estimator from Section 3.1 and the variance correction from Section 3.2, we describe how to obtain posterior samples from our algorithm with a proper variance. We begin by solving the Lyapunov equation in (13). Recall that $\mathbf{A}^{-1} = \nabla^2 f(\boldsymbol{\Omega}^*)$ for the MLE $\boldsymbol{\Omega}^*$ and $\boldsymbol{\Gamma}$ represents the injected noise of the SDE at $\boldsymbol{\Omega} = \boldsymbol{\Omega}^*$. Based on mixing time and Taylor expansion justifications given by Lemma 3.4 and Proposition 3.5, we approximate the unknown quantities $\boldsymbol{\Sigma}$ and $\boldsymbol{\Omega}^*$ by the covariance and mean of the posterior MCMC samples, respectively. We then define the Cholesky decomposition for the uncorrected and corrected covariance as, $\boldsymbol{\Sigma} = \mathbf{E}^\top \mathbf{E}$ and $\mathbf{A} = \mathbf{F}^\top \mathbf{F}$. The corrected samples can be computed as follows,

$$\boldsymbol{\Theta}_k = \mathbf{G}(\boldsymbol{\Omega}_k - \boldsymbol{\Omega}^*) + \boldsymbol{\Omega}^*, \quad \mathbf{G} = (\mathbf{E}^\top \mathbf{F})^{-1}. \quad (14)$$

The samples $\boldsymbol{\Theta}_k$ then have, asymptotically, the proper mean and covariance (i.e., $\mathbb{V}(\boldsymbol{\Theta}_k) = \mathbf{A}^{-1}$). The algorithm is detailed in Algorithm 1.

To compute the Monte Carlo estimator, we must compute $\nabla \log p(\mathbf{Y}_i, \boldsymbol{\gamma}_{ir} | \boldsymbol{\Omega})$. In general, these gradients can be computed using auto-differentiation, making our method highly generalizable, however in the GLMM setting the gradients are straightforward and are presented here. The gradient with respect to the population regression parameter $\boldsymbol{\beta}$ is,

$$\nabla_{\boldsymbol{\beta}} \log p(\mathbf{Y}_i, \boldsymbol{\gamma}_{ir} | \boldsymbol{\Omega}) = \frac{\mathbf{X}_i^\top (\mathbf{Y}_i - \boldsymbol{\mu}_{ir})}{a(\phi)}, \quad (15)$$

where $\mathbf{X}_i = (\mathbf{x}_{i1}, \dots, \mathbf{x}_{in_i})^\top$ is an $n_i \times p$ dimensional matrix of covariates and $\boldsymbol{\mu}_{ir} = (\mu_{ir1}, \dots, \mu_{irn_i})^\top$ is an n_i -dimensional vector. The subject-specific parameters are introduced through the mean function, $\mu_{irt} = d^{-1}(\theta_{irt})$, where $\theta_{irt} = \mathbf{x}_{it}^\top \boldsymbol{\beta} + \mathbf{z}_{it}^\top \boldsymbol{\gamma}_{ir}$. Note that the gradient in (15) comes from properties of the log-cumulant function, $b(\theta_{irt})$, namely that its derivatives yield moments of the distribution. The gradient with respect to the dispersion parameter can be computed as follows,

$$\nabla_{\phi} \log f(\mathbf{Y}_i, \boldsymbol{\gamma}_{ir} | \boldsymbol{\Omega}) = - \sum_{t=1}^{n_i} \left[\frac{Y_{it} \theta_{irt} - b(\theta_{irt})}{a'(\phi) a(\phi)^2} \right] + c'(Y_{it}, \phi), \quad (16)$$

where $a'(\phi)$ and $c'(Y_{it}, \phi)$ are derivatives with respect to ϕ . The gradient for $\boldsymbol{\Sigma}$ reduces to, $\nabla_{\boldsymbol{\Sigma}} \log f(\mathbf{Y}_i, \boldsymbol{\gamma}_{ir} | \boldsymbol{\Omega}) = \nabla_{\boldsymbol{\Sigma}} \log f(\boldsymbol{\gamma}_{ir} | \boldsymbol{\Sigma})$ and is highly dependent on the distributional assumptions of the subject-specific parameters. In Section 5.1 of the online supplementary materials [5], we compute these gradients for the bivariate Gaussian distribution.

Impact of Biased or Approximate Stochastic Gradients

So far in our discussion, including the theoretical analysis of Section 3.2 and in the description of Algorithm 1, we assumed the availability of *iid* Monte Carlo samples from

Algorithm 1 SGLD with Covariance Correction for GLMM**Require:** $\Omega_0, S, \delta, K, R, \kappa$ Define $\epsilon = S/n^{1+\delta}$ **for** $k \in 1, \dots, K$ **do**Draw $\mathcal{S}_k \sim \mathcal{S}$ **for** $i \in \mathcal{S}_k$ **do**Initialize: γ_{i0} **for** $r \in 1, \dots, R$ **do**Sample γ_{ir} from $p(\gamma_i | \mathbf{Y}_i, \Omega_k)$ Compute $\nabla_{\Omega} \log p(\mathbf{Y}_i, \gamma_{ir} | \Omega_k)$ **end for**Compute $\hat{g}_i(\Omega_k) = \frac{1}{R} \sum_{r=1}^R \nabla_{\Omega} \log p(\mathbf{Y}_i, \gamma_{ir} | \Omega_k)$ **end for**Compute $\hat{h}_{\mathcal{S}_k}(\Omega_k) = \frac{1}{S} \sum_{i \in \mathcal{S}_k} \hat{g}_i(\Omega_k)$ Draw $\eta_k \sim N(0, 2\epsilon \mathbf{I}_d)$ $\Omega_{k+1} \leftarrow \Omega_k - \epsilon \left(\nabla f_0(\Omega_k) + n \hat{h}_{\mathcal{S}_k}(\Omega_k) \right) + \kappa \eta_k$ **end for**Compute posterior mean of unconstrained parameters, Ω^* Compute correction, $\hat{\Psi}(\Omega^*)$ ▷ Computation for $\hat{\Psi}(\Omega)$ is given in Lemma 3.2Compute injected noise, $\Gamma = \Gamma(\Omega^*) = \epsilon n^2 \hat{\Psi}(\Omega^*) / (2S) + \kappa \mathbf{I}_d$ Compute inflated posterior variance of Ω , Σ Solve Lyapunov equation to find corrected posterior variance, \mathbf{A}^{-1} Obtain corrected samples Θ_k ▷ Definition of Θ_k is given in (14)

the conditional distribution of latent effects $p(\gamma_i | \mathbf{Y}_i, \Omega)$. The key here is that doing so results in both an unbiased estimator of the population gradient $h_{[n]}(\Omega)$ and a known covariance formula, as shown in Lemma 3.2. Situations in which this is possible are limited, and the feasibility of developing such a high-accuracy sampler heavily depends on the specific form of functions in (15) and (16). Below, we offer two examples in which exact sampling of γ_i is possible.

1. *Linear mixed models (LMMs).* The simplest example would be when $a(\cdot), b(\cdot)$ are identity functions in (15)–(16). $p(\gamma_i | \mathbf{Y}_i, \Omega)$ is then a tractable Gaussian distribution. The methods developed in this work are mostly extraneous for the purpose of LMMs, as the gradients can be vastly simplified to only involve known quantities.
2. *Binary regression with probit link.* In a less simple scenario, we can consider a binary regression model for each $Y_{it} \in \{0, 1\}$ with no dispersion parameter. While the logit link function: $b(\theta) = e^\theta / (1 + e^\theta)$, is most popular in the frequentist literature, probit link function: $b(\theta) = \Phi(\theta)$ for a standard normal CDF Φ , is also commonly used in Bayesian literature. In this situation, the results of [15] can be used to draw exact samples from $p(\gamma_i | \mathbf{Y}_i, \Omega)$, as the density belongs to a family of unified skew-normal distributions proposed by [3]. Extensions of this result to multinomial and tobit likelihoods have since been also derived [16, 2].

An important computational caveat is that the possibility of exact sampling relies on a rejection sampler for high-dimensional truncated normal distributions [8]. In our context, the worst-case dimension for the sampler is $\max_{i=1,2,\dots,n} n_i$, the largest number of within-subject measurements. When this quantity is bounded by a moderately large number (e.g., 100), empirical results from [8] suggest the sampler remains numerically stable. The assumption that the size of most within-unit observations is small is well justified for various biomedical applications, where, despite the large number of patients, the number of longitudinal or spatial measurements available for a single patient is relatively small.

For all other models, such as binary regression with a logit link or Poisson/negative binomial regression, there are currently no methods both easy and generally applicable to draw samples from the conditional distribution $p(\gamma_i|\mathbf{Y}_i, \Omega)$. One can then resort to using inexact samples, whose distribution approximates $p(\gamma_i|\mathbf{Y}_i, \Omega)$, through an “inner loop” MCMC. Concretely, one can now consider an MCMC-based stochastic gradient in (8), which is the ergodic average of a Markov chain, with marginal distributions $\hat{p}^{(r)}(\cdot|\mathbf{Y}_i, \Omega)$ at each step r and ergodic with respect to $p(\gamma_i|\mathbf{Y}_i, \Omega)$:

$$\hat{g}_i^{MCMC}(\Omega) = -\frac{1}{R} \sum_{r=1}^R \nabla \log p(\mathbf{Y}_i, \gamma_{ir}|\Omega), \quad \gamma_{ir} \sim \hat{p}^{(r)}(\gamma_i|\mathbf{Y}_i, \Omega), \quad r = 1, 2, \dots, R.$$

This new, MCMC-based stochastic gradient estimator can be used in Algorithm 1; however, it is no longer unbiased, and the covariance formula derived in Lemma 3.1 is not correct anymore. Hence, a major theoretical concern here is the invalidity of our asymptotic justifications for the correction in Section 3.2, as they assume the use of exact samples from $p(\gamma_i|\mathbf{Y}_i, \Omega)$. A fully rigorous analysis will have to consider an SGLD algorithm with an “inner loop” operation, where for each Ω , a further Markov chain for γ_i is run for a fixed length to evaluate the stochastic gradient. If we can somehow tightly control the Wasserstein distance:

$$\sup_{\Omega} W_2(\hat{p}^{(r)}(\gamma_i|\mathbf{Y}_i, \Omega), p(\gamma_i|\mathbf{Y}_i, \Omega)),$$

for all sufficiently large r , then we can still show the covariance of \hat{g}_i^{MCMC} is similar to that given in Lemma 3.2, up to some remainder diminishing in the length of the “inner loop chain” R . Such a fully rigorous analysis is a formidable challenge, due to the requisite uniformity in Ω , either over the whole \mathbb{R}^d or a sufficiently large set. Since it is impractical to assume the practitioner will choose R varying in different values of Ω , or increasing in n , simple coupling arguments like those of [10] are no longer useful for obtaining ergodicity and mixing rates of the overall SGLD iterates. Furthermore, the technical estimates of any such analysis will apparently depend on the exact nature of the MCMC operations used to draw samples of γ_i ’s, and it is unclear whether generic properties, such as geometric ergodicity, will be useful enough.

On the other hand, while the above concerns are legitimate, we demonstrate in Sections 4 and 5 that any error introduced to the variance of stochastic gradient estimator due to the use of MCMC is negligible for reasonable choices of MCMC samplers targeting $p(\gamma_i|\mathbf{Y}_i, \Omega)$. For instance, in a binary regression model with logit link, we have

consistently used a Gibbs sampler based on Pólya-Gamma data augmentation [31], which was shown to be uniformly ergodic [14]. The resulting SGLD sample variance, corrected according to Algorithm 1, remained close to the true posterior variance, or its approximation using a full-batch MCMC, even when the number of MCMC samples used to approximate the stochastic gradients was moderate ($R = 1,000$). The correction procedure also yielded good approximation of the posterior covariance for a Poisson likelihood model experiments when we used the Metropolis-Hastings proposal (see the supplementary materials [5]).

Finally, while we do not cover other possibilities in our empirical results in the next Section, MCMC is not the only option in approximating $\hat{g}_i(\Omega)$ from (8). First, when each n_i is relatively small, importance sampling using the prior can also work. Our primitive experiments (unreported here) suggest that the prior can be a good enough proposal when $\max_i n_i \leq 10$ and the likelihood model is a good fit to the data, but more sophisticated proposals can help otherwise. If done judiciously, replacing the random number generators by quasi-Monte Carlo points can lead to a faster rate of convergence [22]. Second, since (7) is an integral with respect to the density of $\gamma_i | \mathbf{Y}_i, \Omega$, we can use deterministic approximations. While naive Gauss quadrature methods scale poorly in the dimension of γ_i , alternatives like integrated Laplace approximation [18] or expectation propagation [21] can be attractive, especially so because they tend to yield a better approximation of the targeted integral for a larger amount of data (n_i). Thus, they may complement the use of high-accuracy samplers or importance sampling schemes described above in applications where each independent unit consists of very long trajectories or high-dimensional spatial measurements. We leave these other options for future research and focus on the use of MCMC for the rest of this work.

4 Simulations

In this section, we demonstrate the performance of Algorithm 1 in various GLMM settings. We show that our algorithm properly estimates the posterior mean and variance and is a viable technique when the sample size becomes large, in contrast to existing methods, including Gibbs sampling and a control-variate SGLD. We begin by establishing our algorithm for the linear mixed model. We then apply our model to a logistic regression with random effects. We demonstrate that our algorithm allows for proper inference for GLMMs, even for large n where standard inference algorithms falter.

4.1 Gaussian with Fixed Variance Components

For our first simulation, we investigated the performance of Algorithm 1 in estimating various quantities of the posterior distribution. Data was generated from a linear mixed model, $Y_{it} \stackrel{ind}{\sim} \mathcal{N}(\mathbf{x}_{it}\beta + \mathbf{x}_{it}\gamma_i, \sigma^2)$ and $\gamma_i | \Sigma \stackrel{iid}{\sim} \mathcal{N}(\mathbf{0}, \Sigma)$ with Σ and σ^2 fixed. Since the likelihood is Gaussian, the following quantities can be found in closed form: posterior for β , gradient of the marginal log-likelihood, and posterior predictive distribution (PPD). We assumed $\mathbf{x}_{it} = (1, x_{it})^\top$ and $x_{it} \stackrel{iid}{\sim} \mathcal{N}(0, 1)$ and true parameters, $\beta = (1.5, -0.5)^\top$,

$\sigma^2 = 2$ and $\boldsymbol{\Sigma} = \begin{pmatrix} 1.5 & -0.25 \\ -0.25 & 1.5 \end{pmatrix}$. We analyzed sample sizes of $n \in \{10^2, 10^3\}$, and set $n_i = 10$. For each value of n , we simulated 100 data sets. We used Algorithm 1 to sample from the posterior of β and present results for both the corrected (Θ) and uncorrected (Ω) posterior samples. We used the true data generating model as our likelihood and placed a weakly informative prior on β_j , $\beta_j \stackrel{iid}{\sim} \mathcal{N}(0, 10^2)$ for $j = 0, 1$. We present results for $S \in \{1, 5, 10\}$ and $\delta = \{\delta : \delta \in ([10]/10) \cap \epsilon = S/n^{1+\delta} < n^{-1}\}$. Throughout this simulation $R = 100$. The algorithm ran for 100 continuous time steps (i.e., $100/\epsilon$) and was thinned to 5,000 samples.

Results from this simulation are presented in Figures 1 and 2 and Figures 1, 2 and 3 of the online supplementary materials [5]. In Figure 1, the log posterior variance is presented as a mean with 95% quantile intervals across the 100 simulated data sets. The results are presented for both the uncorrected and corrected samples and across S , n , and parameters (β_0, β_1) and appropriate values of δ . The results indicate that the uncorrected SGLD algorithm consistently overestimated the posterior variance with estimation improving as $\delta \rightarrow 1$. As expected, when $\delta = 1$ the uncorrected SGLD properly estimated the posterior variance. Meanwhile the corrected SGLD had improved performance with quantile intervals that always include the true log variance, and the estimation improved with larger n , S , and δ . These results indicate that choosing a δ value in the middle of the range of possible δ values yields proper variance estimation. Results for posterior mean estimation are presented in online supplementary Figure 1 [5], where it can be seen that the posterior mean can be estimated properly using both the corrected and uncorrected SGLD.

Next, we explored estimation of the moments of the PPD. In Figure 2, we demonstrate the log ratio of the estimated PPD variance using either the corrected or uncorrected SGLD algorithm compared to the true PPD variance. Log ratio values near zero indicate good performance. The results are again presented across S and n and averaged across the n_i observations of $\mathbf{Y}_{i'}$. From this figure, we can see that the corrected SGLD maintains proper uncertainty quantification in the PPD in every simulation setting. The uncorrected SGLD algorithm generally performs poorly, with acceptable performance only when $\delta \rightarrow 1$. As a reminder, SGLD requires longer runtime with larger δ and when the sample size grows values of δ close to 1 are not computationally feasible. Thus, the corrected SGLD is a viable alternative to uncorrected SGLD when the sample size becomes large, because it can yield proper PPD estimation regardless of δ , and therefore is computationally efficient.

Additional results for this simulation are available in the online supplementary materials [5]. In Figure 2 of the online supplementary materials, we present traceplots and density estimates for an example simulated data set to visualize the posterior variance correction. Finally, in Figure 3 of the online supplementary materials, we present evidence that the Monte Carlo estimator does a good job of estimating the true gradient of the marginal log-likelihood (which is available in closed form in this simulation).

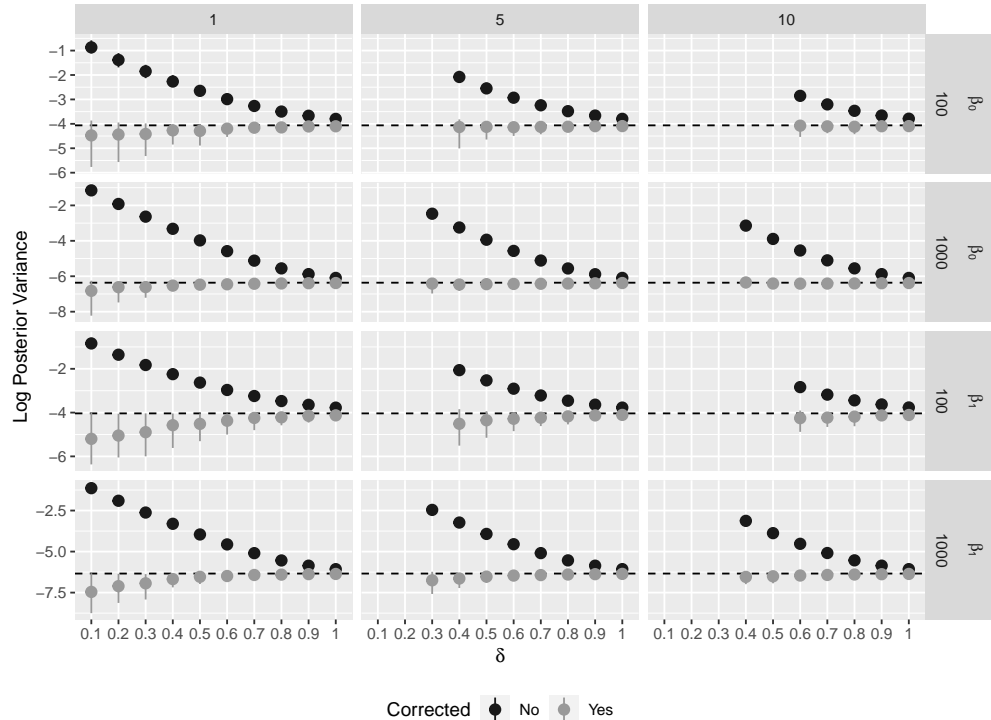


Figure 1: Posterior estimation of the log variance for uncorrected (black) and corrected (grey) SGLD algorithm. Each value represents the mean and 95% quantile intervals based on 100 simulated data sets. The columns represent the minibatch size (S) and the rows represent the sample size (n) and parameter. The black dashed lines indicate the true log posterior variance. Estimates are given across an appropriate range of δ .

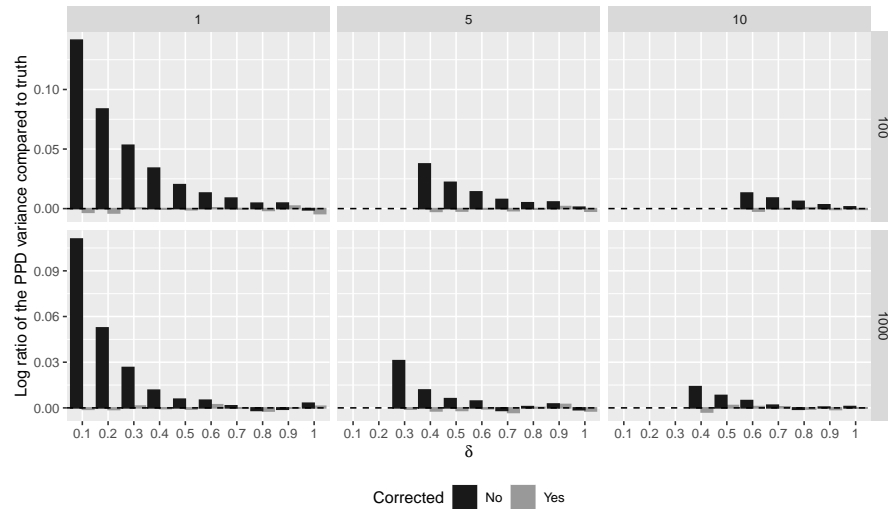


Figure 2: Assessing the algorithm's ability to estimate the variance of the posterior predictive distribution (PPD). Presented are the log ratio of the estimated PPD variance and the true PPD variance for both the uncorrected (black) and corrected (grey) algorithms. Columns and rows indicate batch size (S) and sample size (n), respectively. Black dashed lines indicate correct PPD variance estimation. Estimates are given across a range of δ .

4.2 GLMM with Unknown Variance Components

In this section, we present simulations where the variance and dispersion parameters are unknown. In the main manuscript, we present results for the Bernoulli distribution, while results for Gaussian and Poisson are reserved for the online supplementary materials [5]. The results across all distributions consistently demonstrated the utility of our algorithm.

The Bernoulli GLMM (i.e., logistic regression) is obtained from the exponential family through the following specification, $a(\phi) = 1$, $b(\theta_{it}) = \log(1 + \exp\{\theta_{it}\})$, $c(Y_{it}, \phi) = 0$, $\phi = 1$, and $\theta_{it} = \log(\pi_{it}/(1 - \pi_{it}))$. The mean parameter is given by $\mu_{it} = \pi_{it} = \exp\{\theta_{it}\}/(1 + \exp\{\theta_{it}\})$. This yields the model, $Y_{it}|\gamma_i, \Omega \stackrel{iid}{\sim} \text{Bernoulli}(\pi_{it})$, $\text{logit}(\pi_{it}) = \mathbf{x}_{it}^\top \boldsymbol{\beta} + \mathbf{z}_{it}^\top \boldsymbol{\gamma}_i$, where $\text{logit}(x) = \log(x/(1 - x))$, and the population parameters are given by, $\Omega = \{\boldsymbol{\beta}, \boldsymbol{\Sigma}\}$. We assumed that $\mathbf{x}_{it} = (1, x_{it})^\top$ and $x_{it} \stackrel{iid}{\sim} \mathcal{N}(0, 1)$. True parameters values are the same as in Section 4.1. We examined performance for large samples sizes, $n \in \{10^4, 10^5\}$.

We presented results for both the corrected and uncorrected SGLD algorithms for minibatch sizes of $S \in \{1, 5, 10\}$. For each S we chose a δ using the following definition, $\delta = (\delta_{\min} + \delta_{\max})/2$, where $\delta_{\min} = \min_{\delta} \{\epsilon < n^{-1}\}$ and $\delta_{\max} = 1$ (recall that $\epsilon = n^{-(1+\delta)}S$). The intuition behind this definition is that an ideal value of δ will be in a range with proper posterior variance estimation while maximizing computational efficiency. From Figure 1 it is clear that δ in the middle of the range of possible δ values satisfies these two criteria.

To compare models fairly, we assessed performance as a function of runtime and ran each model for six hours. Performance was evaluated as convergence to the proper posterior mean and variance. Since the true posterior distribution was no longer available, we compared performance to Gibbs sampling. We also considered the SGLD-CV algorithm proposed by [4], a variant of SGLD algorithm using control variates. The algorithm requires an additional, preparatory SGD step to approximately locate the posterior mode, from which the SGLD algorithm is initialized. To make comparisons to SGLD-CV in the GLMM setting required adapting it to account for the intractable marginal log-likelihood, so we used Fisher's identity (5) and MCMC samples for each $\boldsymbol{\gamma}_i$, outlined below. It is not straightforward whether the theoretical properties of their algorithm extend to our current GLMM setting. Empirically, we observed that a choice of step-size proportional to $O(1/n)$ in the SGD and sampling step quickly leads to divergent iterates in some of the model parameters. For the simulations below, we fixed the step-size of the SGLD-CV algorithm to be $O(1/n^{1+\delta})$ with $\delta = 0.4$.

To estimate the Monte Carlo gradient, requires $\nabla_{\Omega} \log p(\mathbf{Y}_i, \gamma_{ir} | \Omega)$ with respect to each of the unconstrained parameters. Throughout this simulation, we assumed a bivariate Gaussian for the subject-specific parameters, $p(\boldsymbol{\gamma}_i | \boldsymbol{\Sigma}) = \mathcal{N}(\mathbf{0}, \boldsymbol{\Sigma})$, where $\boldsymbol{\Sigma}$ is parameterized by the variances for the subject-specific intercept (σ_1^2) and slope (σ_2^2), and the correlation (ρ). We performed inference using the unconstrained parameters, $\delta_1 = \log(\sigma_1)$, $\delta_2 = \log(\sigma_2)$, and $\delta_\rho = \log((\rho + 1)/(1 - \rho))$. Finally, for each of the standard deviations, σ_k ($k = 1, 2$), we placed a half-t distribution with degree-of-freedom parameter ν and scale s . We placed a uniform prior for ρ , $\rho \sim \text{Uniform}(-1, 1)$. We

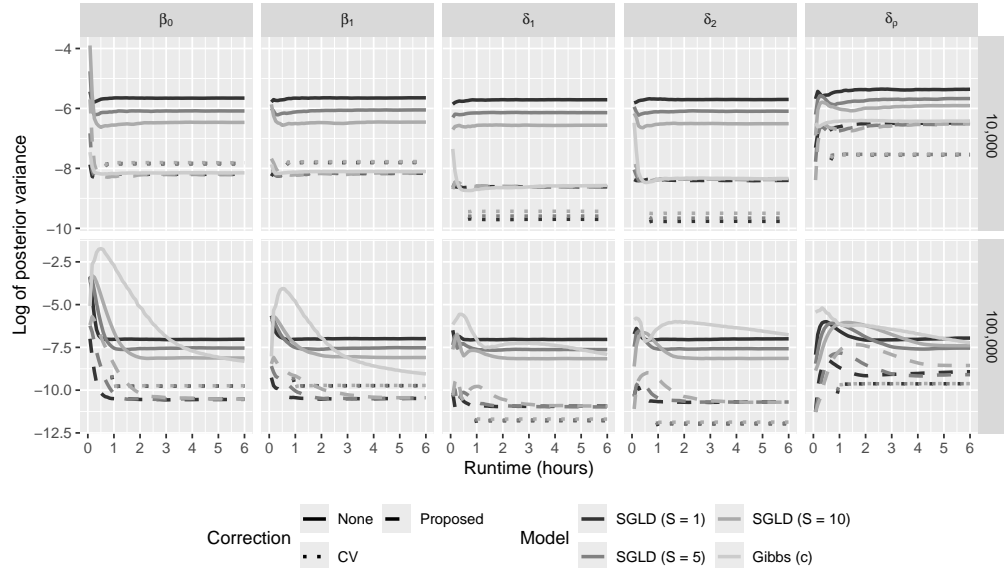


Figure 3: Log of posterior variance estimates presented across runtime (hours) for the Bernoulli GLMM model. Columns and rows indicate parameter and sample size (n), respectively. Algorithms include conditional (c) Gibbs sampling and the SGLD algorithm with various batch sizes (S). Thee variants of the SGLD are presented: vanilla SGLD (solid); SGLD initialized using the control variates algorithm by [4], adapted to GLMMs (dashed); and SGLD samples corrected according to our proposal (long dashed). At each point in time, the log posterior variance was calculated using the most recent 75% of the samples up to that point. Estimates are averaged across 100 simulated data sets.

placed a weakly informative prior on $\beta, \beta \sim \mathcal{N}(\mathbf{0}_p, \sigma_\beta^2 \mathbf{I}_p)$ with $\sigma_\beta^2 = 100$. Gradients for the conditional log-likelihood and prior and are reported in online supplementary Section 5.1 [5]. Finally, to compute our Monte Carlo estimator we required samples from $p(\gamma_i | \mathbf{Y}_i, \Omega)$. In online supplementary Section 5.2.1 [5] we derived a Gibbs sampler using Pólya-Gamma data augmentation. Due to increased complexity, $R = 1,000$. For the SGLD-CV algorithm, we used $R = 5,000$ so that, albeit the computational complexity is initially increased, our competitor algorithm has a better chance of accurately locating the posterior mode. Details for the Gibbs sampler for the Bernoulli are given in Section 5.2.2 of the online supplementary materials [5].

The results for this simulation are presented in Figure 3 for the posterior variance. Results for the posterior mean are reserved for the online supplementary materials [5], since no correction is needed. Figure 3 presents posterior estimation of the variance on log scale. We cannot compare the performance to a true variance nor can we compare to the true data generating parameter values, so in this simulation the comparator

becomes the Gibbs sampler (which is unbiased although computationally challenged). We presented results for both the corrected (solid line), uncorrected (dashed line), and control variate (dotted line) SGLD algorithms. To make the comparisons fair, corrections were computed during runtime, meaning $\hat{\Psi}(\Omega)$ was estimated dynamically. There are three main takeaways from this figure: (1) the corrected SGLD algorithm yielded posterior variance estimates that were the same as the Gibbs sampler algorithms, while the uncorrected SGLD algorithm overestimated the variance; (2) the performance of the corrected SGLD algorithm was not impacted by the increase in sample size, as opposed to the Gibbs samplers whose estimation worsened; and, (3) the competitor algorithm SGLD-CV, overestimated the posterior variance for the regression coefficients (β_0, β_1) and underestimated the random effect variance parameters $(\delta_1, \delta_2, \delta_\rho)$. Importantly, these takeaways were true regardless of S and δ , and furthermore these results were consistent for the population regression parameters (β) , and variance parameters (Σ) .

Particularly interesting among these phenomena is the way in which SGLD-CV incorrectly estimates the posterior variance. An inflated posterior variance estimate for β_0, β_1 may be explained by the fact that a naive adaptation of SGLD-CV to use the GLMM likelihood, unlike our proposed correction, does not correct for the additional variability of the stochastic gradient induced by using MCMC samples to approximate the gradient of the marginal log-likelihood. It is more puzzling that the SGLD-CV underestimates the posterior variance for the entries of Σ , for which we do not have a satisfying theoretical explanation. We emphasize that this deflation of variance is as undesirable as inflation, possibly more so because the algorithm will mislead us to overconfidence about the parameter estimates. The core message of this comparison is that GLMMs with big data require tailored methods for calibrating uncertainty.

Figures 4, 5, 6, 7 and 8 in the online supplementary materials present simulation results for the Bernoulli mean, plus the Gaussian, and Poisson posterior mean and variance [5]. These results are consistent with the Bernoulli results, and indicate the utility of our algorithm across GLMM settings.

5 Real World Data Analysis

In patients with ophthalmic disorders, psychiatric risk factors play an important role in morbidity and mortality. Understanding how patient characteristics impact the probability of a patient having distress is a critical task that will facilitate proper and early psychiatric screening and result in prompt intervention to mitigate its impact. In this analysis of real world clinical data, we analyzed data from the Duke Ophthalmic Registry, a database that consists of adults at least 18 years of age who were evaluated at the Duke Eye Center or its satellite clinics from 2012 to 2021. The goal of the analysis was to identify patient characteristics associated with a diagnosis of psychiatric distress upon each clinic encounter. The Duke University Institutional Review Board approved this study with a waiver of informed consent due to the retrospective nature of this work. All methods adhered to the tenets of the Declaration of Helsinki for research involving human subjects and were conducted in accordance with regulations of the Health Insurance Portability and Accountability Act.

We defined $Y_{it} \in \{0, 1\}$ as an indicator of psychiatric distress for patient i ($i \in [n]$) and encounter t ($t \in [n_i]$). Distress was defined using an electronic health records phenotype that has been detailed previously [6]. Each encounter was observed at follow-up time τ_{it} , where $\tau_{i1} = 0$, such that τ_{it} for $t > 1$ indicates the number of years from baseline encounter. The encounters for each patient were collected in the vector \mathbf{Y}_i . We also defined an indicator $w_i = 1 (\sum_{t=1}^{n_i} Y_{it} = 0)$ to indicate whether all observations for a patient were zero. The observed data is given by (\mathbf{Y}_i, w_i) with the joint distribution $p(\mathbf{Y}_i, w_i) = p(w_i)p(\mathbf{Y}_i|w_i)$. The outcome was modeled as $Y_{it} \stackrel{ind}{\sim} \text{Bernoulli}(\pi_{it})$, with $\text{logit}(\pi_{it}) = \mathbf{x}_{it}^\top \boldsymbol{\beta} + \mathbf{z}_{it}^\top \boldsymbol{\gamma}_i$ and the missing indicator was modeled as $w_i \stackrel{ind}{\sim} \text{Bernoulli}(p_i)$, where $\text{logit}(p_i) = \alpha_0 + \mathbf{x}_i^\top \boldsymbol{\alpha}_{-0}$ and $\boldsymbol{\alpha} = (\alpha_0, \boldsymbol{\alpha}_{-0}^\top)^\top$. The covariates were defined as follows, $\mathbf{x}_{it} = (1, \tau_{it}, \mathbf{x}_i^\top)$, where \mathbf{x}_i contains patient-level covariates (e.g., baseline age). The vector $\mathbf{z}_{it} = (1, \tau_{it})^\top$ inducing a subject-specific intercept and slope for follow-up time, such that $q = 2$.

The set of population parameters is $\boldsymbol{\Omega} = (\boldsymbol{\alpha}, \boldsymbol{\beta}, \boldsymbol{\Sigma})$ and the posterior distribution is, $p(\boldsymbol{\Omega}|\mathbf{Y}, \mathbf{w}) \propto p(\boldsymbol{\Omega}) \prod_{i=1}^n p(w_i|\boldsymbol{\alpha}) \int p(\mathbf{Y}_i|\boldsymbol{\gamma}_i, w_i, \boldsymbol{\beta}) p(\boldsymbol{\gamma}_i|\boldsymbol{\Sigma}) d\boldsymbol{\gamma}_i$, with corresponding gradient,

$$\nabla \log p(\boldsymbol{\Omega}|\mathbf{Y}, \mathbf{w}) = \nabla \log p(\boldsymbol{\Omega}) + \sum_{i=1}^n \nabla \log p(w_i|\boldsymbol{\alpha}) + \mathbb{E}_{\boldsymbol{\gamma}_i|\mathbf{Y}_i, w_i, \boldsymbol{\Omega}} [\nabla \log p(\mathbf{Y}_i, \boldsymbol{\gamma}_i|w_i, \boldsymbol{\Omega})],$$

where the expectation can be approximated using (8). The gradients inside of the expectation are $\nabla_{\boldsymbol{\beta}} \log p(\mathbf{Y}_i|\boldsymbol{\gamma}_{ir}, \boldsymbol{\beta}, w_i) = 1(w_i = 0) \nabla_{\boldsymbol{\beta}} \log p(\mathbf{Y}_i|\boldsymbol{\gamma}_{ir}, \boldsymbol{\beta})$, $\nabla_{\boldsymbol{\Sigma}} \log p(\boldsymbol{\gamma}_{ir}|\boldsymbol{\Sigma})$ is defined as before and $\nabla_{\boldsymbol{\alpha}} \log p(w_i|\boldsymbol{\alpha}) = (w_i - p_i) \mathbf{x}_i^\top$. Samples of $\boldsymbol{\gamma}_{ir}$ can be obtained from $p(\boldsymbol{\gamma}_i|\mathbf{Y}_i, w_i, \boldsymbol{\Omega}) = w_i p(\boldsymbol{\gamma}_i|\boldsymbol{\Sigma}) + (1 - w_i) p(\boldsymbol{\gamma}_i|\mathbf{Y}_i, \boldsymbol{\Omega})$. It is clear that when $w_i = 1$ the posterior is equal to the prior and when $w_i = 0$ the posterior is the same as the Bernoulli GLMM.

The sample included 40,326 patients (n), of which 15% had at least one distress indicator. On average patients had 9 encounters, were 60 years of age, 41% male, and 68% white. Full demographic details are given in Table 1 of the online supplementary materials [5]. In our model, the reference categories for categorical variables were white (Race), and commercial (Insurance). The continuous variables age, income, and education were standardized.

We performed inference using both the corrected and uncorrected SGLD algorithms using $S = 1$. In Figure 4, we presented odds ratios and 95% credible intervals for $\boldsymbol{\beta}$ for both SGLD algorithms. Estimates are color-coded to indicate whether the 95% credible interval included one, which corresponds to a one-sided Bayesian p-value. Of the variables, other race, drugs use, Medicaid insurance, Medicare insurance, single marital status, and smoking were all significantly associated with an increased probability of being distressed, assuming the presence of any distress (i.e., $w_i = 1$). An increase in baseline age, African American/black race, increased follow-up time, Hispanic/Latino ethnicity, and Asian race were all associated with a decreased probability of being distressed. Examination of this figure illustrates the importance of the covariance correction for obtaining proper inference as the uncorrected SGLD algorithm yielded insignificant p-values for Medicaid insurance, Medicare insurance, and Hispanic/Latino ethnicity.

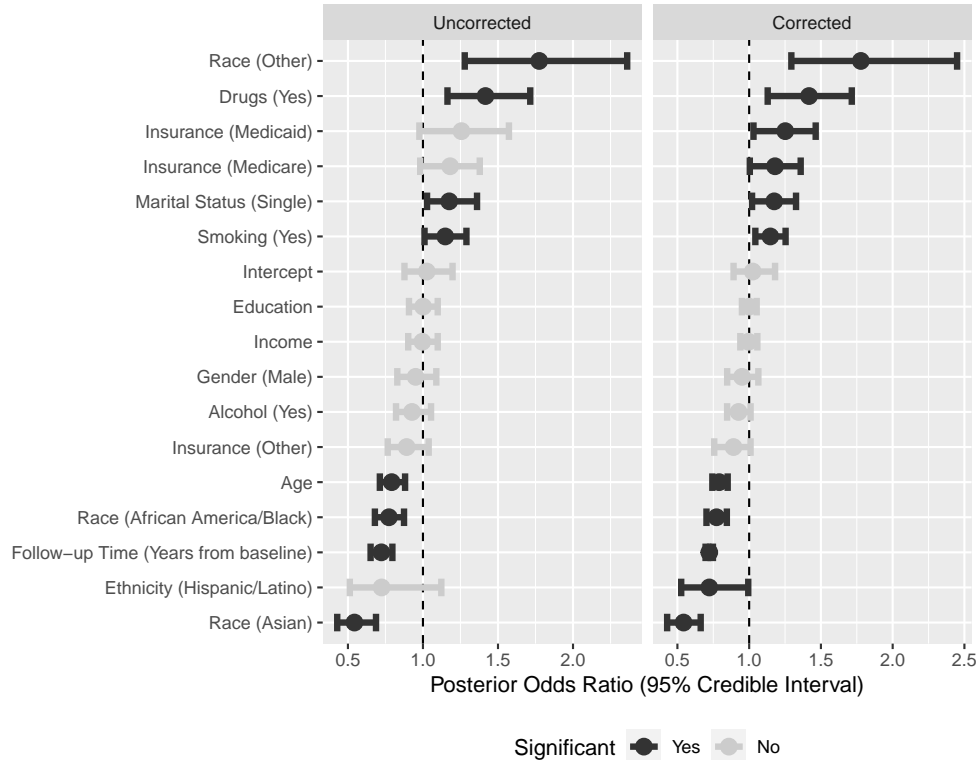


Figure 4: Posterior odds ratios and 95% credible intervals for β . Summaries are presented for the uncorrected and corrected SGLD algorithm. The parameters are presented in decreasing order and color coded based on whether the credible interval contained zero.

The posterior estimates of α and Σ are given in Figure 8 and Table 2 of the online supplementary materials [5].

6 Discussion

In this paper, we introduced an algorithm for performing accurate and scalable Bayesian inference for the GLMM in the large-sample regime. To the best of our knowledge, our approach is the first to adapt SGMCMC methods to this setting, overcoming limitations that arise from a naive application of such algorithms to dependent data. The main contributions of our work include: (i) a Monte Carlo approximation of the gradient of the marginal log-likelihood using Fisher's identity, enabling SGMCMC updates in the presence of intractable integrals; and (ii) an asymptotic analysis of the variance

structure of the resulting algorithm, allowing us to derive a post-hoc correction that restores the correct posterior covariance. Together, these contributions enable scalable and reliable Bayesian inference for GLMMs, yielding posterior samples with appropriate mean and variance, even in complex dependent-data settings.

We demonstrated the accuracy and scalability of our algorithm for Bayesian inference in GLMMs through a series of simulation studies in Section 4. In Section 4.1, we focused on the linear mixed model with fixed variance components, allowing us to directly evaluate the algorithm’s ability to recover the true posterior distribution, the gradient of the marginal log-likelihood, and the PPD. As shown in Figure 1, our algorithm accurately recovers the posterior variance, in contrast to the uncorrected SGLD algorithm, with performance improving as S , n , and δ increase. These results indicate that our method captures the full posterior distribution, enabling valid statistical inference, including hypothesis testing and prediction. To assess predictive performance, we examined the moments of the PPD. Figure 2 displays the log ratio of PPD variances relative to the truth for both corrected and uncorrected SGLD; our method provides properly calibrated predictive uncertainty. In Section 4.2, we extended the evaluation to general GLMMs with Bernoulli, Gaussian, and Poisson outcomes. Across these settings, our algorithm consistently matched the posterior mean and variance estimated by Gibbs sampling while maintaining computational efficiency as n increased, even in regimes where MCMC becomes prohibitively expensive.

As discussed in the introduction, fixed step-size SGLD leads to inflated posterior variance [10], and a variety of correction strategies have been developed to address this, including preconditioning [34], Metropolis-Hastings adjustments [20], and control variate methods [4]. However, these approaches are typically designed for independent data settings and can be prohibitively expensive or difficult to extend to models with intractable marginal likelihoods, such as GLMMs. In our simulations, we compared our method directly to the SGLD-CV method, a scalable method with good theoretical properties. While SGLD-CV effectively reduces variance from minibatching, it fails to account for the additional variability introduced by approximating the marginal likelihood. This omission results in miscalibrated posterior uncertainty in GLMMs. In contrast, our correction accounts for both sources of variability and achieves accurate uncertainty quantification, as demonstrated in both posterior and predictive comparisons across a range of GLMM settings. These results highlight the importance of tailoring variance correction to the specific structure and inferential challenges of dependent-data models.

In Section 5, we applied our algorithm to a real-world electronic health records dataset to demonstrate its utility for statistical inference in complex, large-scale settings. As shown in Figure 4, the covariance correction meaningfully impacted inference: 95% credible intervals changed interpretation for key covariates such as insurance status and ethnicity, underscoring the importance of properly accounting for variance inflation. These results depend on Assumption 1 in the online supplementary materials [5], and in the presence of model misspecification, which is nearly inevitable in real data, we expect additional variability in the injected noise. This may explain why the observed correction scaling in Figure 4 was more modest than the $n^{-\delta} \approx 10^{-2}$ predicted in the well-specified

regime. Extending our method to better accommodate model misspecification remains an important direction for future work and may be key to broadening its applicability in practice.

Finally, the current limitations of this work opens up numerous avenues for future research. The primary difficulty in studying the effectiveness of our method under different scenarios is that for many GLMMs, deriving an unbiased estimator of the gradient is almost always unfeasible. While our work has addressed the issue by using MCMC draws, this additional layer of approximation renders the stochastic gradient biased and with a possibly inflated variance. We have justified the validity of our asymptotic correction for using MCMC draws through an empirical success of our algorithm, applied to simulations and real-world data. Nevertheless, a better understanding of the method in the future will require a finer study of the bias and variance induced by the use of MCMC, and whether alternative approximation schemes perform better under different settings. We highlight that the lack of unbiased estimator for the gradient renders fitting GLMMs a challenging task, regardless of whether Bayesian estimation is used, and the question of best practices for different GLMMs remains an open research problem. For instance, recent results [11] reported inaccuracies of methods like penalized quasi-likelihood, in general, and Laplace approximation, when the random effects are sparse. Such concerns have sparked interests in approximating MLE through more modern techniques, like expectation propagation [21]. Synergizing this literature with our current framework, to obtain computational strategies tailored to yield smaller variance of the stochastic gradient for different models, will be an interesting and important avenue of research for practitioners.

There are other limitations and possible improvements. At a theoretical level, future research directions include obtaining quantitative concentration bounds for the uncorrected posterior distribution, thereby giving indications on how to choose the parameter δ depending on n . Also, it will be important to consider extensions of our algorithm to modern machine learning settings, to incorporate momentum in stochastic gradient updates, provide guarantees for high-dimensional models, and infer deep neural networks. At a methodological level, future research directions include generalizations allowing for various distributional assumptions and covariance specifications for the subject-specific parameters, flexible prior specification for the population regression parameter to allow for sparsity and regularization, and extensions to accommodate time series, spatial data, and federated learning.

Acknowledgments

We would like to acknowledge the late Sayan Mukherjee, whose thoughtfulness, generosity, and intellectual vision were instrumental in bringing together the authors of this work. Sayan had a remarkable ability to unite collaborators from very different backgrounds to tackle challenging and important problems, and this project is a direct reflection of that gift. His insight and encouragement shaped the direction of this work, and we are deeply grateful for his contributions and for the opportunity to have worked with him.

Funding

Research reported in this publication was supported by the National Eye Institute of the National Institutes of Health (Bethesda, Maryland) under Awards Number R00EY033027 (SIB). The sponsor or funding organization had no role in the design or conduct of this research. The content is solely the responsibility of the authors and does not necessarily represent the official views of the National Institutes of Health. AA is member of INdAM (GNAMPA group), and acknowledges partial support of Dipartimento di Eccellenza, UNIPI, the Future of Artificial Intelligence Research (FAIR) foundation (WP2), PRIN project ConStRAINeD, PRA Project APRiSE, and GNAMPA Project CUP_E53C22001930001.

Supplementary Material

Supplementary material to ‘Scalable Bayesian Inference for Generalized Linear Mixed Models via Stochastic Gradient MCMC’. The supplementary materials contain derivations, additional simulation and data analysis results, and Gibbs sampling details.

References

- [1] Agresti, A. (2012). *Categorical Data Analysis*, Volume 792. John Wiley & Sons. [1](#)
- [2] Anceschi, N., A. Fasano, D. Durante, and G. Zanella (2023). Bayesian conjugacy in probit, tobit, multinomial probit and extensions: A review and new results. *Journal of the American Statistical Association* 118(542), 1451–1469. [12](#)
- [3] Arellano-Valle, R. B., M. D. Branco, and M. G. Genton (2006). A unified view on skewed distributions arising from selections. *Canadian Journal of Statistics* 34(4), 581–601. [12](#)
- [4] Baker, J., P. Fearnhead, E. B. Fox, and C. Nemeth (2019). Control variates for stochastic gradient MCMC. *Statistics and Computing* 29, 599–615. [2](#), [18](#), [19](#), [23](#)
- [5] Berchuck, S. I., Y. Baek, F. A. Medeiros, and A. Agazzi (2025). Supplementary material to “Scalable Bayesian Inference for Generalized Linear Mixed Models via Stochastic Gradient MCMC.” DOI:10.1214/[provided by typesetter]. [7](#), [8](#), [10](#), [11](#), [14](#), [15](#), [18](#), [19](#), [20](#), [21](#), [22](#), [23](#)
- [6] Berchuck, S. I., A. A. Jammal, D. Page, T. J. Somers, and F. A. Medeiros (2022). A Framework for Automating Psychiatric Distress Screening in Ophthalmology Clinics Using an EHR-Derived AI Algorithm. *Translational Vision Science & Technology* 11(10), 6–6. [21](#)
- [7] Booth, J. G. and J. P. Hobert (1999). Maximizing generalized linear mixed model likelihoods with an automated monte carlo em algorithm. *Journal of the Royal Statistical Society Series B: Statistical Methodology* 61(1), 265–285. [3](#)
- [8] Botev, Z. I. (2017). The normal law under linear restrictions: simulation and estimation via minimax tilting. *Journal of the Royal Statistical Society Series B: Statistical Methodology* 79(1), 125–148. [13](#)

- [9] Breslow, N. E. and D. G. Clayton (1993). Approximate inference in generalized linear mixed models. *Journal of the American Statistical Association* 88(421), 9–25. [1](#), [3](#)
- [10] Brosse, N., A. Durmus, and E. Moulines (2018). The promises and pitfalls of stochastic gradient Langevin dynamics. *Advances in Neural Information Processing Systems* 31, 1–11. [2](#), [4](#), [9](#), [10](#), [13](#), [23](#)
- [11] Capanu, M., M. Gönen, and C. B. Begg (2013). An assessment of estimation methods for generalized linear mixed models with binary outcomes. *Statistics in medicine* 32(26), 4550–4566. [24](#)
- [12] Chen, T., E. Fox, and C. Guestrin (2014). Stochastic gradient Hamiltonian Monte Carlo. In *International Conference on Machine Learning*, pp. 1683–1691. PMLR. [2](#)
- [13] Chib, S. (1995). Marginal likelihood from the gibbs output. *Journal of the American Statistical Association* 90(432), 1313–1321. [3](#)
- [14] Choi, H. M. and J. P. Hobert (2013). The polya-gamma gibbs sampler for bayesian logistic regression is uniformly ergodic. *Electronic Journal of Statistics* 7, 2054–2064. [14](#)
- [15] Durante, D. (2019). Conjugate bayes for probit regression via unified skew-normal distributions. *Biometrika* 106(4), 765–779. [12](#)
- [16] Fasano, A. and D. Durante (2022). A class of conjugate priors for multinomial probit models which includes the multivariate normal one. *Journal of Machine Learning Research* 23(30), 1–26. [12](#)
- [17] Fisher, R. A. (1925). Theory of Statistical Estimation. In *Mathematical Proceedings of the Cambridge Philosophical Society*, Volume 22, pp. 700–725. Cambridge University Press. [3](#), [5](#)
- [18] Fong, Y., H. Rue, and J. Wakefield (2010). Bayesian inference for generalized linear mixed models. *Biostatistics* 11(3), 397–412. [14](#)
- [19] Frühwirth-Schnatter, S. (2004). Estimating marginal likelihoods for mixture and markov switching models using bridge sampling techniques. *The Econometrics Journal* 7(1), 143–167. [3](#)
- [20] Gelman, A., J. B. Carlin, H. S. Stern, and D. B. Rubin (1995). *Bayesian Data Analysis*. Chapman and Hall/CRC. [2](#), [3](#), [23](#)
- [21] Hall, P., I. Johnstone, J. Ormerod, M. Wand, and J. Yu (2020). Fast and accurate binary response mixed model analysis via expectation propagation. *Journal of the American Statistical Association* 115(532), 1902–1916. [14](#), [24](#)
- [22] He, Z., Z. Zheng, and X. Wang (2023). On the error rate of importance sampling with randomized quasi-monte carlo. *SIAM Journal on Numerical Analysis* 61(2), 515–538. [14](#)
- [23] Jasra, A., K. J. Law, and D. Lu (2021). Unbiased estimation of the gradient of the log-likelihood in inverse problems. *Statistics and Computing* 31(3), 1–18. [5](#)

- [24] Kantas, N., A. Doucet, S. Singh, J. Maciejowski, and N. Chopin (2015). On Particle Methods for Parameter Estimation in State-Space Models. *Statistical Science* 30(3), 328–351. [5](#)
- [25] Li, C., C. Chen, D. Carlson, and L. Carin (2016). Preconditioned stochastic gradient Langevin dynamics for deep neural networks. In *Proceedings of the AAAI Conference on Artificial Intelligence*, Volume 30. [2](#)
- [26] Ma, Y.-A., T. Chen, and E. Fox (2015). A complete recipe for stochastic gradient MCMC. *Advances in Neural Information Processing Systems* 28, 1–9. [2](#)
- [27] Naylor, J. C. and A. F. Smith (1982). Applications of a method for the efficient computation of posterior distributions. *Journal of the Royal Statistical Society Series C: Applied Statistics* 31(3), 214–225. [3](#)
- [28] Nemeth, C. and P. Fearnhead (2021). Stochastic gradient Markov chain Monte Carlo. *Journal of the American Statistical Association* 116(533), 433–450. [2](#)
- [29] Ormerod, J. T. and M. P. Wand (2012). Gaussian variational approximate inference for generalized linear mixed models. *Journal of Computational and Graphical Statistics* 21(1), 2–17. [3](#)
- [30] Patterson, S. and Y. W. Teh (2013). Stochastic gradient Riemannian Langevin dynamics on the probability simplex. *Advances in Neural Information Processing Systems* 26, 1–9. [2](#)
- [31] Polson, N. G., J. G. Scott, and J. Windle (2013). Bayesian inference for logistic models using Pólya–Gamma latent variables. *Journal of the American Statistical Association* 108(504), 1339–1349. [14](#)
- [32] Rue, H., A. Riebler, S. H. Sørbye, J. B. Illian, D. P. Simpson, and F. K. Lindgren (2017). Bayesian computing with INLA: A review. *Annual Review of Statistics and Its Application* 4, 395–421. [3](#)
- [33] Segal, M. and E. Weinstein (1989). A new method for evaluating the log-likelihood gradient, the Hessian, and the Fisher information matrix for linear dynamic systems. *IEEE Transactions on Information Theory* 35(3), 682–687. [5](#)
- [34] Stephan, M., M. D. Hoffman, D. M. Blei, et al. (2017). Stochastic gradient descent as approximate Bayesian inference. *Journal of Machine Learning Research* 18(134), 1–35. [2](#), [23](#)
- [35] Tan, L. S. L. and D. J. Nott (2013). Variational Inference for Generalized Linear Mixed Models Using Partially Noncentered Parametrizations. *Statistical Science* 28(2), 168–188. [3](#)
- [36] Teh, Y., A. Thiéry, and S. Vollmer (2016). Consistency and fluctuations for stochastic gradient Langevin dynamics. *Journal of Machine Learning Research* 17, 1–33. [2](#)
- [37] Tierney, L., R. E. Kass, and J. B. Kadane (1989). Fully exponential Laplace approximations to expectations and variances of nonpositive functions. *Journal of the American Statistical Association* 84(407), 710–716. [3](#)

- [38] Tran, M.-N., N. Nguyen, D. Nott, and R. Kohn (2020). Bayesian deep net GLM and GLMM. *Journal of Computational and Graphical Statistics* 29(1), 97–113. [3](#), [5](#), [6](#)
- [39] Vollmer, S. J., K. C. Zygalakis, and Y. W. Teh (2016). Exploration of the (non-) asymptotic bias and variance of stochastic gradient Langevin dynamics. *The Journal of Machine Learning Research* 17(1), 5504–5548. [2](#)
- [40] Welling, M. and Y. W. Teh (2011). Bayesian learning via stochastic gradient Langevin dynamics. In *Proceedings of the 28th international conference on machine learning (ICML-11)*, pp. 681–688. [2](#), [4](#), [6](#)